ORIGINAL ARTICLE

Erosion wear behavior of spark plasma-sintered Ti-6Al-4V reinforced with TiN nanoparticles

Mokgoba Glodean Kganakga[1] · German Prieto[2] · Oluwasegun Eso Falodun[1] · Walter R. Tuckart[2] · Babatunde Abiodun Obadele[3] · Olarewaju Olawale Ajibola[4] · Peter Apata Olubambi[1]

Abstract

The extensive application of titanium alloys is delimited as their erosion wear properties deteriorate when exposed to erosive and harsh environments. The present research investigates the effects of TiN additions (2, 4, and 6 vol.%) on the Ti-6Al-4V alloy prepared by spark plasma sintering technique. Erosion wear behaviour of the composites was investigated by high-velocity solid particle erosion test and tribometer pin-on-disc friction module method. The duration of the test was 10 min, while the mass loss of the sample was recorded after 2-min interval. The surface analysis and phase identifications of the sintered composites were examined by optical microscopy (OM), scanning electron microscopy (SEM), and X-ray diffraction (XRD), respectively. Microstructural analysis revealed a transformation from lamellar with β grain boundaries in Ti-6Al-4V alloy to bimodal structures upon addition of TiN nanoparticles. XRD patterns of the alloy indicated an increase in diffraction peaks from lower intensity to high intensity with an increase in TiN nanoparticle content. Erosion is visible in Ti-6Al-4V alloy, 4 and 6 vol.% TiN, but less severe with 2 vol.% TiN addition for all the test times. However, this is due to grain detachment of the hard phase regions between the matrix and the reinforcing phase of the composites. The results showed the presence of micro-voids on the eroded surfaces. It was found that Ti-6Al-4V alloy with TiN nanoparticle addition was resistant to erosion wear, while the recorded steady-state friction coefficients for all the samples range from 0.2 to 0.4. However, an increase in microhardness values ranges from 342 to 513 $HV_{0.1}$.

Keywords Ti-6Al-4V alloy · TiN nanoparticle · Metal matrix composites · Erosion · Wear

1 Introduction

Titanium alloys remains a class of material that offers outstanding properties, which makes them chosen over other materials in different applications such as aerospace, biomedical, and other engineering fields [1]. Ti-6Al-4V alloys also known as the workhorse of the titanium industry are used for structural materials owing to their excellent mechanical properties which are characterized by high strength to weight ratio, high corrosion resistance, and low thermal expansion [2].

However, it is quite evident that titanium alloys are faced with several challenges of erosion and wear due to combustion system and environmental factors occurring at high temperatures [3]. It stated that atmospheric situation like volcano ashes, sandstorms, and ice particles induce erosion and wear damage on aero-engines [4]. Erosion resistance is a significant thought in structuring many fundamental components made out of Ti-6Al-4V alloy, for example, the blades and disks of aeroplane compressors and gas turbines [5, 6]. Titanium and its alloys do not have high protection from erosive wear as a result of the generally low surface hardness [7, 8]. The most extensive technique to deal with improving the mechanical properties of titanium alloys is strengthening mechanism with the reinforcement of secondary phases (ceramic particles) to attain more hardness and strength [9–11]. Nevertheless,

✉ Oluwasegun Eso Falodun
   segzy201@gmail.com

1   Centre for Nanomechanics and Tribocorrosion, University of Johannesburg, Johannesburg, South Africa

2   Tribology Group, Engineering Department, Universidad Nacional del Sur, CONICET, Bahía Blanca, Argentina

3   Department of Chemical, Materials and Metallurgical Engineering, Botswana International University of Science and Technology, Palapye, Botswana

4   Department of Materials and Metallurgical Engineering, Federal University, Oye, Ekiti, Nigeria

various ceramic materials have been used as the reinforcement phase for titanium alloys to study the influence on physical and mechanical properties [12, 13]. Introducing and reinforcing a metal matrix with ceramic particles stand as a pinning effect, a strong barrier for the movement of dislocations within inside the grains and interface between the grains [14, 15]. The processing method toward intensifying the matrix and reinforcement boundary plays a significant role in determining the influence on the strength of the metal matrix composites [16, 17].

Erosion wear can be described as a removal of material from the target material due to impacting solid particles on the surface caused by mechanical interaction [18]. These frequently arise at the surface of titanium parts, which is a significant cause for failure that restricts the lifetime of components during service [19]. It has been seen that the effects of high-velocity particles on a substrate can instigate local harm like scratching, melting, extruding, and propagation of crack formation. These wear conditions rely upon a few boundaries like substrate and erodent material, impacting angle, disintegration time, particle velocity, temperature, and atmosphere [4]. Different factors likewise affecting erosion wear are erodent hardness, size, shape, velocity, impact angle, testing conditions like temperature, and relative wetness. These are characterized by ploughing, gouging, and pitting on the material surface [20]. One of the properties of an erosive wear-resistant material is high hardness and strength. It is worth noting that titanium alloys exhibit relatively low surface hardness and consequently they possess low wear resistance [21]. Hardness of a material depends on how the material has been hardened and the material composition. Material with high hardness value possesses high wear resistance [20]. In this regard, TiN nanoceramic was used as a reinforcement material to improve the hardness and wear properties of Ti-6Al-4V alloy due to its outstanding mechanical properties such as high hardness and strength [22]. By virtue of their small grain sizes, nanocrystalline materials have high wear resistance attributed to their high hardness and strength. Small grain sizes delimit the traditional dislocation activities such as tangling, pileup formation, and forest interactions by allowing plastic deformation to occur being dominated by new mechanisms [23].

Avcu et al. [24] studied solid particle erosion behavior of Ti6Al4V alloys and found that erosion rate increases by increases in particle velocities and decreases by increases in erodent particle size. Sahoo et al. research on effect of microstructural variation on erosion wear behavior of Ti-6Al-4V alloy and report that among all four control factors, impact velocity was the most significant controlling factor influencing the solid particle erosion wear of Ti-6Al-4V alloy, followed by impact angle, microstructural features, and size of erodent [6]. On that note, different processing techniques were used to amplify the erosive wear and physical and chemical depositions have been used to improve the erosion resistance

of the alloy [25]. However, these methods become extricated as their protection of the material surface was too shallow and resulted in deterioration in erosion wear properties.

Metal matrix composites relate to the severity and reinforced with ceramic material provided by a metal matrix [26]. Titanium and its alloys are widely used in MMC production to improve its properties for usage in high-temperature environments. However, the interface between the matrix and the reinforcement is the critical region that is influenced during the production process. If there is an inappropriate interface, it can prompt the limiting of the composite properties. The issues related with the interfaces are the interfacial relation, degradation of the reinforcement phase, and deficit of wettability with the matrix phase [27]. Among these, the most significant method to improve interfacial properties is spark plasma sintering which was identified as a suitable method to reinforce composite materials, to produce a homogenous and high strength composite. Spark plasma sintering (SPS) is a relatively novel powder metallurgical technique, which requires less sintering time. SPS could produce near net shape products, and fully dense microstructure with no grain growth thereby controlling the microstructure and remain close to its original grain size which further improved the mechanical properties of the finished product [28, 29]. The process of sintering at higher temperatures and holding time tend to promote the formation and growth of new phases in sintered matrix composites [30]. Thus, in this study, spark plasma sintering was used to consolidate Ti-6Al-4V alloy with nanoceramic TiN, and further examine the erosive wear behavior of titanium-based composites reinforced with nanoceramic TiN which was tested using high-velocity solid particle erosion test.

2 Experimental procedure

2.1 Material and composite production

Titanium matrix composites used for this study were developed from Ti-6Al-4V alloys as the main matrix while TiN nanoparticle serves as reinforcement phase which was supplied by TLS Technik GmbH & Co., Germany, and Nanostructured & Amorphous Material Inc., TX, USA respectively. The powders were mechanically mixed using a Turbula T2F shaker mixer at a mixing speed of 49 rpm for 8 h in a dry condition for proper dispersion of the composite materials to diffuse in each other. The reinforcement composition was 2, 4, and 6 vol.% TiN nanoparticles.

The admixed powders of different compositions of Ti-6Al-4V alloy and TiN nanoparticle were sintered using spark plasma sintering (SPS) system model HHPD 25 manufactured by FCT, Germany. Ti-6Al-4V-TiN nanocomposites with die dimensions of 40-mm diameter and 5-mm thickness were

produced. The optimized sintering parameters were carried out at a temperature of 1100 °C, the pressure of 50 MPa, a heating rate of 100 °C/min, and holding time of 30 min, which was used to sinter the materials in a vacuum. Metallography analysis was performed by various methods using grinding, polishing, and etching with Kroll's chemical reagent as etchant in order to reveal the microstructure of the sintered titanium matrix composites. Microstructural analysis was performed using field emission scanning electronic microscope (JEOL JSM-7600F) equipped with energy-dispersive x-ray spectroscopy (EDS) and a Zeiss optical microscope. X-ray diffraction was done using a PW1710 Philips diffractometer, with monochromatic Cu target Kα radiation at 40 kV and 40 mA while phase identification was done to identify the constituent phases in the sintered composites. The microhardness test of the sintered composites was characterized using a Vickers tester (FALCON series) on the polished surface under an applied load of 100 gf and dwell time of 15 s at ambient temperature.

2.2 Erosion wear evaluation

In this study, the solid particle erosion tests were conducted using a high-velocity solid erosion test as per ASTM G76 standard. The Ti-6Al-4V alloys with a different fraction of TiN (2, 4, and 6 vol.%) were used to study erosion wear behaviour at room temperature (25 °C). Alumina was used as an erodent particle. The erosion tests were performed at different times which are 2, 5, 8, and 10 min, respectively, at an incident angle of 90° and particle velocity of 20 m/s. Each test was tested at least four times for different testing times. The sintered composites were cleaned using acetone, dried, and weighed to an accuracy of 0.1 mg using an electronic weighing balance before and after each erosion test. The eroded samples were weighed after each test to observe the changes in the weight loss of the sintered composite due to erosion. Wear tracks and wear depth of the eroded surfaces were evaluated using scanning electron microscopy (SEM) and confocal microscopy. Figure 1 shows a pictorial diagram of a solid erosion test which was used to conduct this experiment.
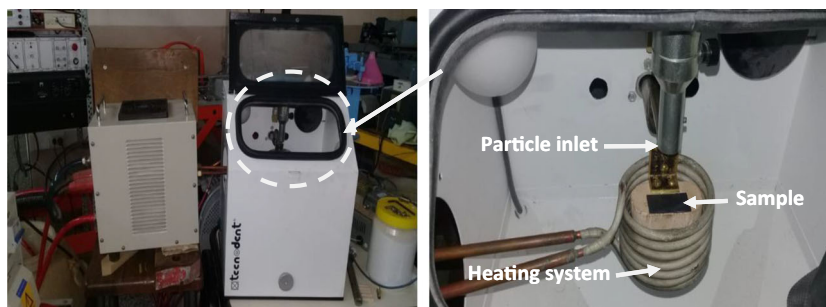
3 Results and discussion

3.1 Microstructure observations

The typical microstructure of Ti-6Al-4V alloy consists of an alternating layer of alpha/beta phases, also known as the lamellar structure [31]. Figure 1a–d show a microstructure of Ti-6Al-4V alloy with and without TiN nanoceramic observed under an optical microscope. In respect to what other researchers have discovered, it was observed that the microstructures were comprised of the alpha/beta phases. The presence of Al and V in titanium has led to the concurrent existence of alpha and beta phases in the microstructure [32]. It was also evidenced that there was a transformation in microstructure from lamellar to a bimodal microstructure as shown in Fig. 2c–d. It is worth noting that there was a reduction in grain size as the microstructure changes from lamellar to biomodal structure. It could be inferred that the reduction in grain size was attributed to the presence of TiN on the grain boundaries [23]. When TiN nanoparticle is added into Ti-6Al-4V alloy, it locates into the grain boundaries, thereby blocking the stepwise movement of dislocation from one grain to another. As a result, the grains are inhibited to grow to larger extends and the resultant microstructures are evidenced.

Figure 3a–d give SEM images of Ti-6Al-4V alloys and those with TiN nanoparticles. The results validate what was already observed through the optical microscope. The images show an alternating layer of alpha and beta phases on the pure Ti-6Al-4V alloys, whereas alloys strengthened with TiN nanoparticle show a relatively homogenous distribution of TiN nanoparticles in the microstructures with interface between the alloy and nanosized particles taking place during spark plasma sintering operation [12]. However, sintering of Ti-6Al-4V over the alpha and beta transformation temperature will bring about grain development regardless of the heating and cooling rates' condition [33]. Figure 4 shows XRD patterns of the alloy indicating an increase in diffraction peaks from lower intensity to high intensity with an increase in TiN content [30, 34] confirmed that the nitrogen which is an alpha stabilizers reacts with Ti, thereby increasing more chances of forming an alpha phase; hence, broader diffraction peaks are

Fig. 1 Typical setup of a high-velocity solid particle erosion test

Fig. 2 Optical micrographs of sintered titanium matrix composites with TiN nanoparticle addition: **a** Ti-6Al-4V alloy, **b** 2 vol.%, **c** 4 vol.%, and **d** 6 vol.%
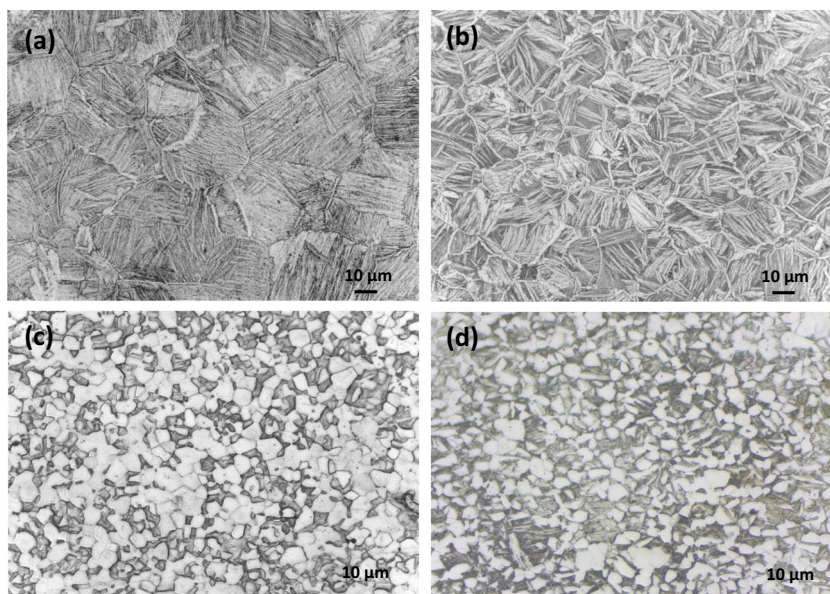
observed as TiN content is increased. However, it was observed that the peaks shift slightly in 2θ diffraction angles which could be attributed to internal stresses generated during spark plasma sintering and X-ray absorption effect [12]. According to Falodun et al. [35], sintering at high temperature causes substantial nitrogen diffusion and consequently prompts phase transformation from TiN to Ti_2N. XRD confirm the presence of α and β phases and no unwanted phases were created. It is indicative of the fact that sintering at a higher temperature above the α-β transus temperature advances some structural and phase evolution of the titanium matrix composites. However, the transformation of TiN to

Ti_2N phase will help to enhance the strength and hardness and prevent deterioration during the use of the composite.

3.2 Volume loss of the sintered composite

In this regard, the erosion wear behaviour of Ti-6Al-4V/TiN composites was evaluated as a function of mass loss against TiN volume fraction. Figure 5 illustrates a diagram of average mass loss versus time. It is apparent that erosion is more pronounced in Ti-6Al-4V with 4 and 6 vol.% TiN, but less severe with 2 vol.% TiN addition for all the test times. These could exhibit that there was grain detachment of the hard phase areas

Fig. 3 SEM micrographs of spark plasma-sintered samples of Ti-6Al-4V alloy with TiN nanoparticle addition: **a** Ti-6Al-4V alloy, **b** 2 vol.%, **c** 4 vol.%, and **d** 6 vol.%
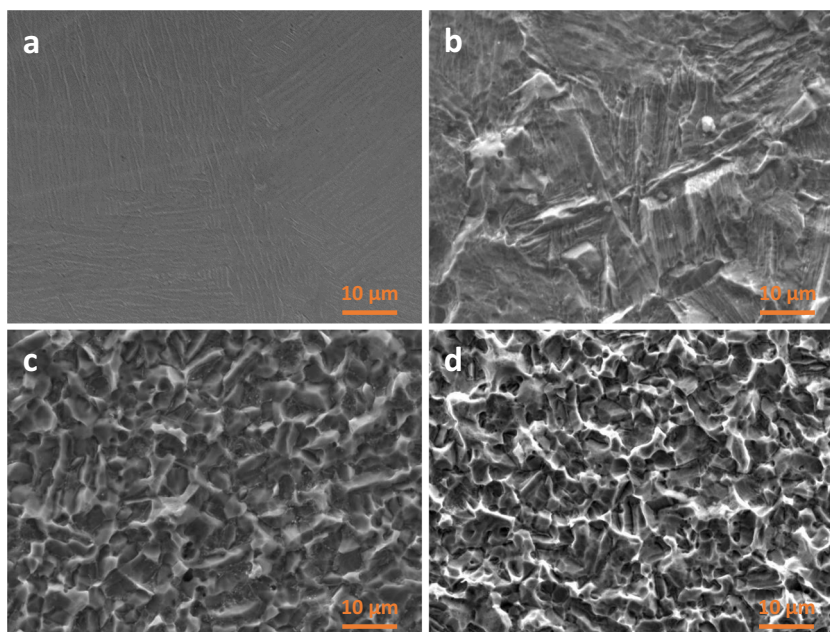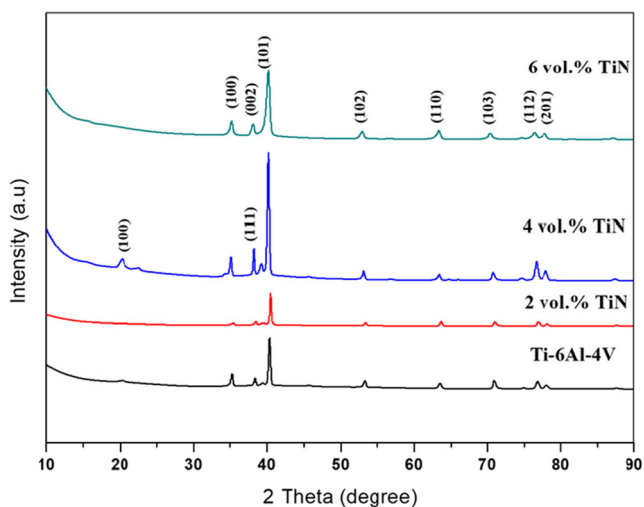
Fig. 4 XRD pattern of spark plasma-sintered titanium matrix composite

dependent on the reinforcement fraction of the composites. Also, samples with higher hard phase reinforcement addition had some porosity. The porosity deteriorates the interfaces between the matrix and the reinforcing phases. The discharge of hard particles can start adding three-body wear mechanisms bringing about severe wear [36]. Russias et al. [37] reported that TiN addition below 6 vol.% improves the mechanical properties while above leads to deterioration in the mechanical properties. However, it was observed that as the nitrogen content goes high, the mechanical properties such as electrical resistivity and heat conduction increase, whereas the hardness decreases [38].
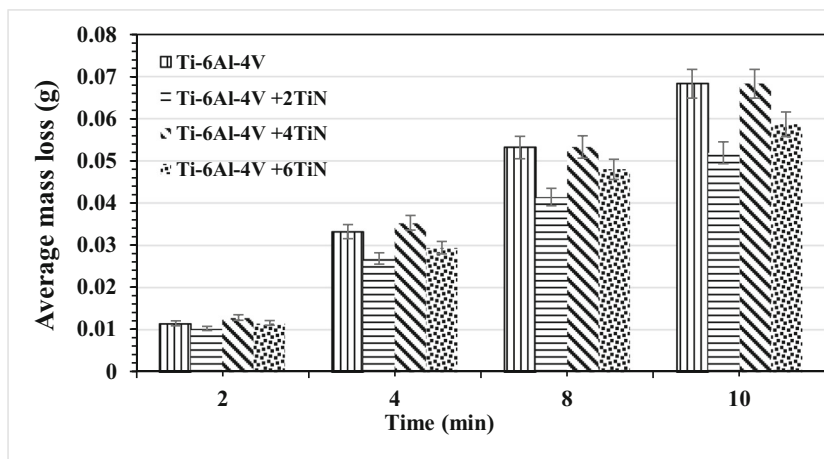
Figure 6 show micrographs of the eroded surfaces of Ti-6Al-4V with TiN nanosized composites at different test times. The microstructure of the eroded surfaces demonstrated circular pits growing outwards the centre with an increase in test time. The estimated final diameter of Ti-6Al-4V alloy was 9.8 mm; then, it reduces to 8.20 mm as the TiN content increases to 2 vol.% TiN. Subsequently, the diameter of the eroded surface expands to 10.63 mm at Ti-6Al-4V + 4 vol.% TiN

then reduces to 10.51 mm at Ti-6Al-4V + 6 vol.% TiN. The erosive wear of metal brought about by plastic distortion was essentially affected by the wear coefficient, the material thickness, the erodent speed, and the hardness [39].

3.3 Erosion surface characterization

Figure 7a–d present the morphology of the eroded surface samples. This study assists in determining the mechanism responsible for the loss of material during the erosion test. Figure 7a–d show that the presence of micro-voids was observed on the eroded surfaces. Several mechanisms contributed to the removal of material during erosion of the titanium composite which includes ploughing, pileup directing to platelet formation and separation, and lip fragmentation which were the primary mechanisms of material loss during the erosion test [5, 6]. However, it was observed that when TiN content increases, erosion was dominated by plastic deformation [18] because erosion mechanisms of composite contain in the plastic deformation of the reinforcement phase and the brittle fracture of ceramic grains [39]. Thus, the process of erosion degrading in composite begins particularly in the reinforcement phase due to the relatively low strength of ceramics [40, 41]. The influence of erodents on the composite causes the strength of affecting particles which has been absorbed by the plastic matrix phase, thereby bringing about the removal of ductile phase [42]. The confocal analysis is represented by a combination of colours. The blue colour represents the lowest depth at which erosion has taken place whereas the red colour shows the surface on which erosion has taken place. Therefore, it can be concluded from the colour coding that erosion wear scar was more dominant in the central zone of the surface and produced slowly outward the surface. This shows a clear pattern of plastic deformation damage including low-angle directional ploughing leading to directional plastic deformation of the surface [43]. Furthermore, erosion was more pronounced in Ti-6Al-4V +

Fig. 5 Weight loss of the sintered titanium matrix composite

Fig. 6 SEM micrographs of the eroded surface at test parameters of 10 min at 90° incident angle: **a** Ti-6Al-4V alloy, **b** 2 vol.% TiN, **c** 4 vol.% TiN, and **d** 6 vol.% TiN
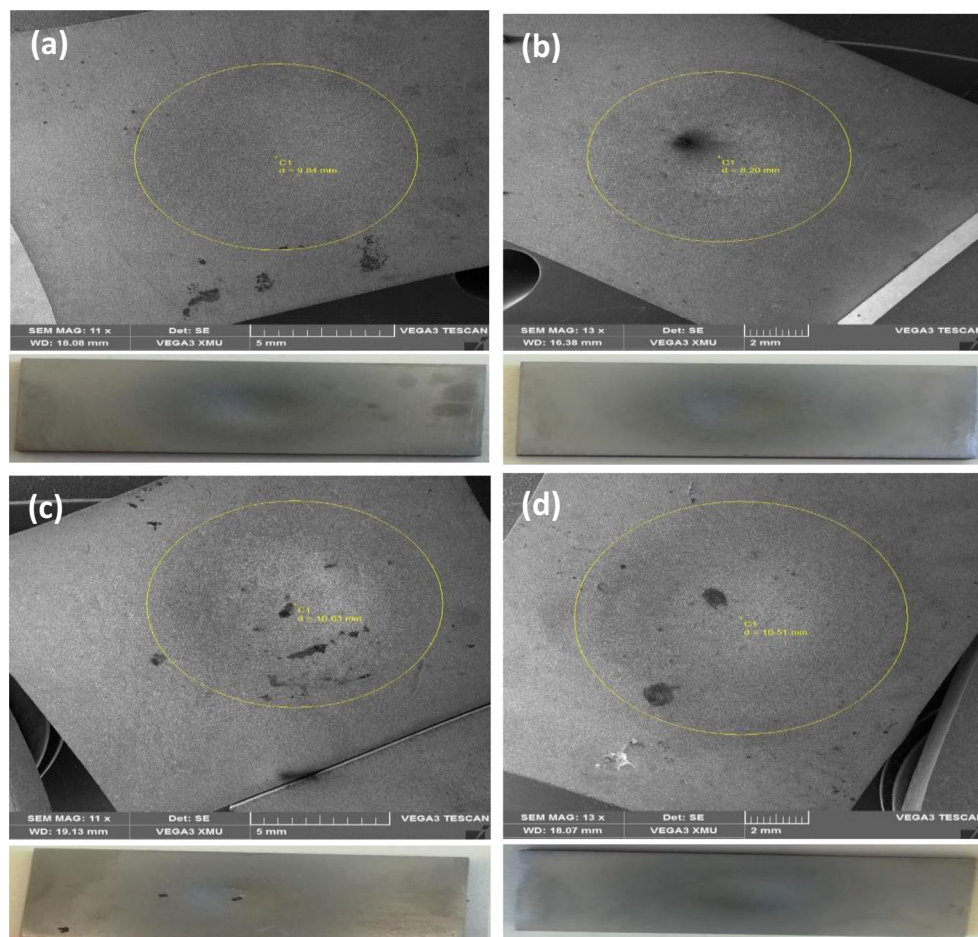
4 vol.% TiN (974.721 μm) and shallower at Ti-6Al-4V + 2 vol.% TiN (933.361 μm).

3.4 Wear behavior of sintered composite

When two bodies slide against each other under applied force, the force opposing the smooth movement of the surfaces is said to be friction force. It depends on the roughness and the material inspected. The reduced friction means the contact between the two surfaces is less, and hence, less wear results. Coefficient of friction can be described as the value obtained when the friction force between two bodies is calculated. Figure 8a–d below distinguishes wear behaviour as a function of coefficient friction against time. It indicates that friction coefficient decreases with TiN content and further increases when the TiN content goes to 6 vol.%. As revealed in Fig. 8a–d, the recorded steady-state friction coefficients for all the samples range from 0.2 to 0.4. This could also be explained by the high percentage mass loss that occurred in Ti-6Al-4V + 6 vol.% TiN when compared with other composites. It is observed that the average mass loss reduces when the TiN volume fraction increases by 2 and 4 vol.% respectively. Subsequently, the fluctuation behavior of the friction

coefficient average mass loss increases when the TiN is increased to 6 vol.%. It could be deduced that the increase in TiN addition improves the wear resistant of Ti-6Al-4V alloy to 4 vol.%, above which the wear properties starts to deteriorate. Review of related literature reported that better wear resistance could be achieved when the introduction of ceramic strengthening is increased as a result of improvement in the composite hardness values. Russias et al. [37] confirmed that addition of TiN improves the mechanical properties upon some certain percentage, and further addition could lead to deterioration in the material properties. The formation and presence of tribolayer causes an increase in the coefficient of friction in Fig. 8d, which hinders real contact to occur within the composite and the counterface material. Also, increase in coefficient of friction could be caused by TiN sticking out from the titanium matrix composite during the contact and sliding against each other by this means increases the coefficient of friction [44].

3.5 Microhardness test

Hardness of a material is defined as the resistant of a material to indentation which load is applied on a given area [45]. It

Fig. 7 SEM micrographs of the eroded titanium matrix composites material with corresponding confocal analysis (**a**) Ti-6Al-4V alloy, (**b**) 2 vol.% TiN, (**c**) 4 vol.% TiN and (**d**) 6 vol.% TiN
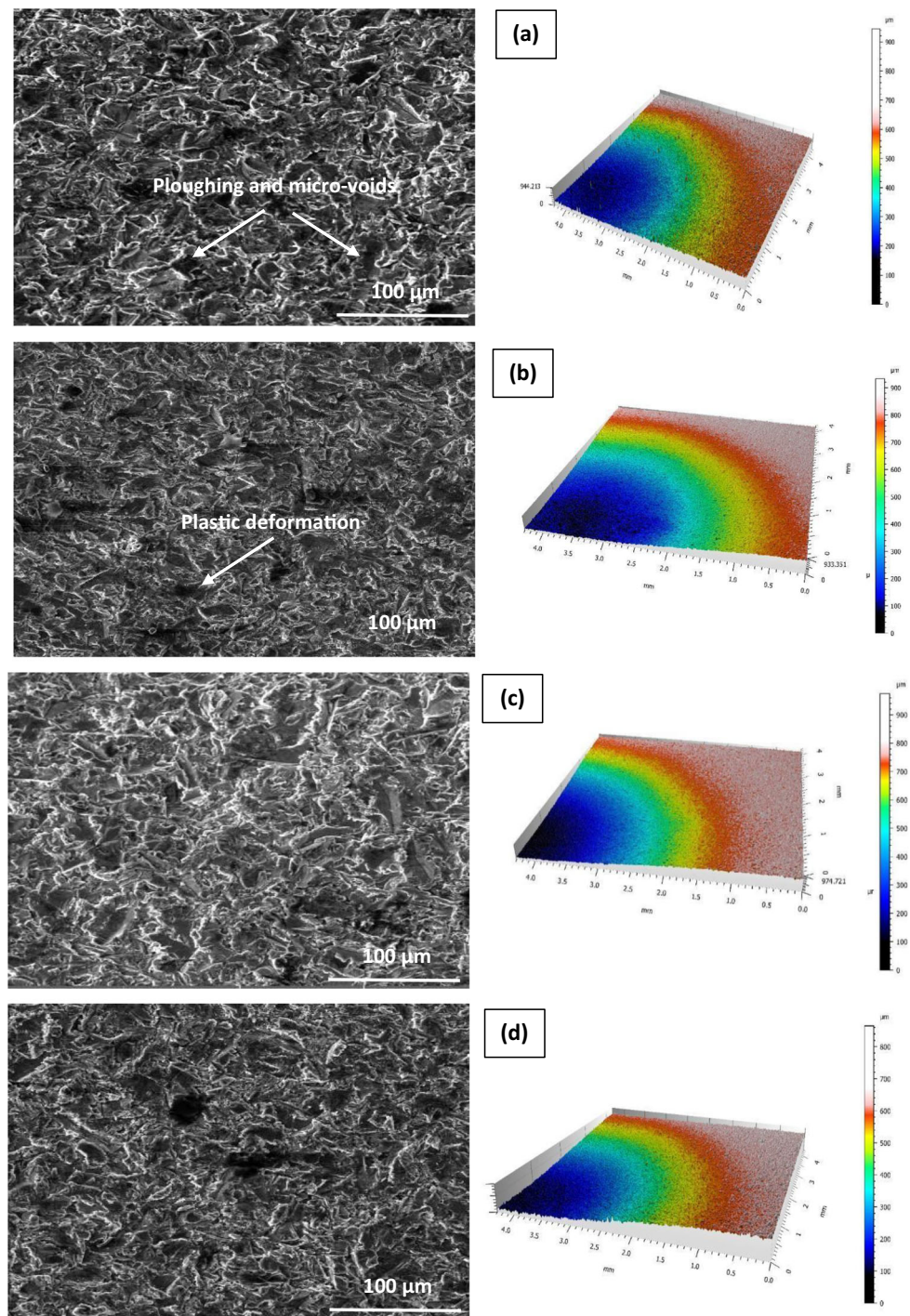
was discovered that hardness is strongly dependent on the physical and structural sizes of a crystalline material. On the other hand, it is worth noting that the morphology of pileups during indentation could cause lower penetration depth and eventually high hardness values [46]. However, in a heterogeneous material, the location of indents in the microstructure determines the final hardness value of a material and it was also stated that at high load will certainly lead to high hardness values [47]. However, high hardness values are mainly due to small grain sizes, which could be attributed to the difficulties with which a dislocation needs to move from one point to another [48, 49]. Generally, the microhardness values of the sintered titanium matrix composites were higher than those of the unreinforced Ti-6Al-4V alloy from 342 to 513 HV0.1.
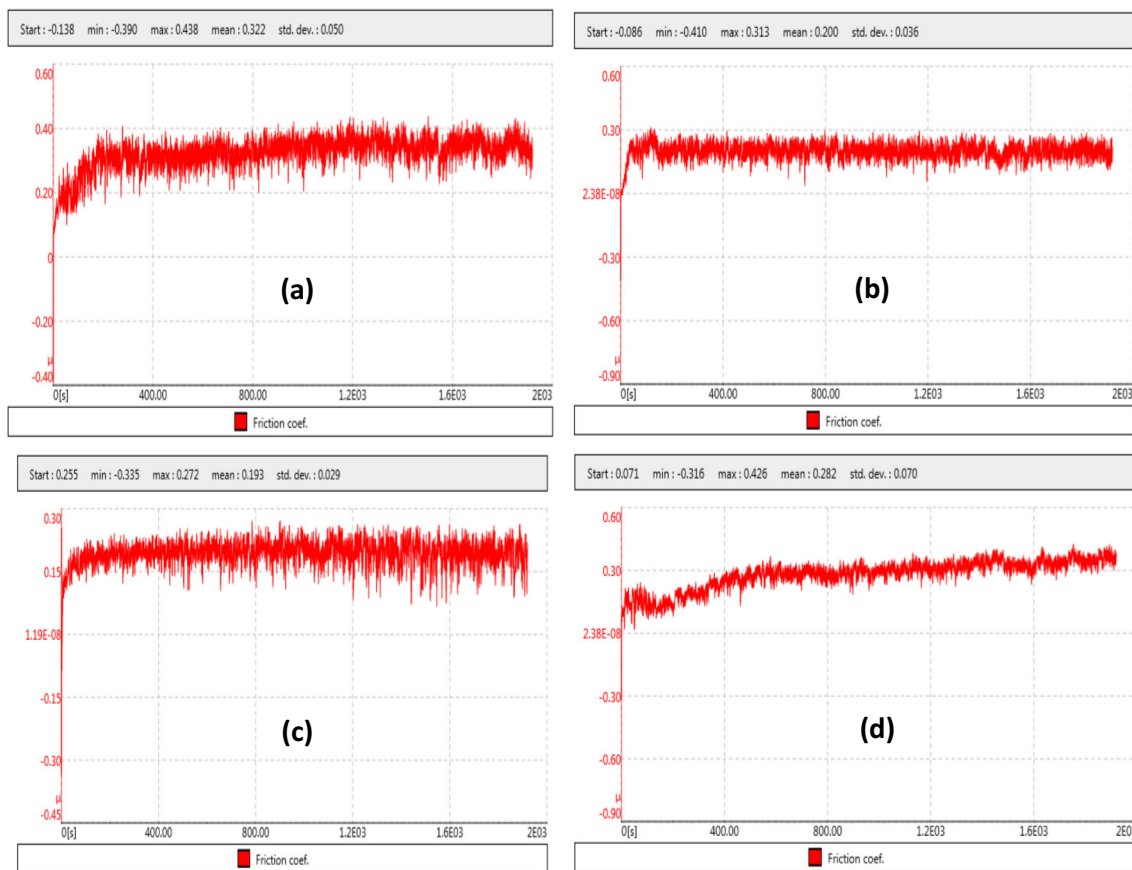
Fig. 8 Coefficient of friction against time of sintered composites: **a** Ti-6Al-4V alloy, **b** 2 vol.% TiN, **c** 4 vol.% TiN, and **d** 6 vol.% TiN

This shows that the addition of TiN nanoparticles certainly improved the hardness of the sintered composites as shown in Table 1. The increase in hardness could be credited to the uniform dispersion of TiN nanoparticles and formation of harder phase (Ti_2N) in Ti-6Al-4V alloy.

4 Conclusion

In this study, the effect of titanium nitride addition on the microstructure, hardness, and erosion wear behaviour of spark plasma-sintered Ti-6Al-4V alloy was investigated. The conclusions were summarized as follows:

Table 1 Hardness values of the sintered composite

Materials	Microhardness ($HV_{0.1}$)
Ti-6Al-4V	342.6
2 vol.% TiN	378.3
4 vol.% TiN	467.8
6 vol.% TiN	513.9

1. The microstructural evolution indicated that the presence of TiN in Ti-6Al-4V led to a transformation from alpha/beta lamellar to bimodal microstructure. The change in microstructure was attributed to TiN nanoparticle on the grain boundary acting as a dislocation barrier, thereby inhibiting grain growth, while XRD patterns of the sintered composite show an increase in diffraction peaks upon addition of TiN nanoparticle content. However, sintering at a temperature above the α-β transus temperature promotes the phase evolution of the titanium matrix composites.

2. In erosion wear, average weight loss of Ti-6Al-4V reduces with an increase TiN up to 2 vol.% TiN; then, an increase at 4 vol.% TiN followed by a decrease at 6 vol.% TiN. The grain detachment of the hard phase areas, which is dependent on the reinforcement fraction of the composites, resulted in the decrease.

3. The diameter of the erosion wear tracks was observed to be increasing with TiN addition. The average eroded surfaces were dominated with ploughing, micro-voids, and pileup directing to platelet formation of the sintered composite material loss during erosion test.

4. There is an indication that coefficient of friction decreases with TiN nanoparticles and further increases when the

TiN content goes to 6 vol.%, which is due to formation and presence of tribolayer that hinders real contact to occur within the counterface use and the composite material.

5. The titanium alloy reinforced with TiN nanoparticles significantly increases the hardness values in the matrix. The main reason for microhardness increase was due to dispersion strengthening and second phase formation, which is of harder phases (Ti_2N) in the titanium matrix composite.

References

1. Falodun OE, Obadele BA, Oke SR et al (2019) Characterization of spark plasma sintered TiN nanoparticle strengthened titanium alloy using EBSD and TKD. Mater Res Bull 117:90–95

2. Donachie MJ (2000) Titanium: a technical guide. ASM international

3. Sharma SK, Selokar AW, Kumar BVM, Venkateswaran T (2017) High temperature erosion behavior of spark plasma sintered ZrB2-SiC composites. Ceram Int 43:8982–8988

4. Naveed M, Renteria AF, Nebel D, Weiß S (2015) Study of high velocity solid particle erosion behaviour of Ti2AlC MAX phase coatings. Wear 342:391–397

5. Yerramareddy S, Bahadur S (1991) Effect of operational variables, microstructure and mechanical properties on the erosion of Ti-6Al-4V. Wear 142:253–263

6. Sahoo R, Mantry S, Sahoo TK, Mishra S, Jha BB (2013) Effect of microstructural variation on erosion wear behavior of Ti-6Al-4V alloy. Tribol Trans 56:555–560

7. Lisiecki A (2015) Titanium matrix composite Ti/TiN produced by diode laser gas nitriding. Metals (Basel) 5:54–69

8. Laguna-Camacho JR, Escalante-Martínez JE, Cruz-Vicencio R et al (2014) Solid particle erosion behaviour of TiN coating on AISI 4140 steel. J Surf Eng Mater Adv Technol 2014. https://doi.org/10.4236/jsemat.2014.41001

9. Choi B-J, Sung S-Y, Kim M-G, Kim Y-J (2008) Evaluation the properties of titanium matrix composites by melting route synthesis. J Mater Sci Technol 24:105

10. Abkowitz S, Abkowitz SM, Fisher H, Schwartz PJ (2004) CermeTi® discontinuously reinforced Ti-matrix composites: manufacturing, properties, and applications. Jom 56:37–41

11. Falodun OE, Obadele BA, Oke SR, Okoro AM, Olubambi PA (2019) Titanium-based matrix composites reinforced with particulate, microstructure, and mechanical properties using spark plasma sintering technique: a review. Int J Adv Manuf Technol 102:1689–1701

12. Falodun OE, Obadele BA, Oke SR, Ige OO, Olubambi PA (2020) Effect of TiN and TiCN additions on spark plasma sintered Ti–6Al–4 V. Part Sci Technol 38:156–165

13. Zhang Z, Shen X-B, Wen S, Luo J, Lee SK, Wang FC (2010) In situ reaction synthesis of Ti–TiB composites containing high volume fraction of TiB by spark plasma sintering process. J Alloys Compd 503:145–150

14. Mazahery A, Shabani MO (2013) Plasticity and microstructure of A356 matrix nano composites. J King Saud Univ Sci 25:41–48

15. Monazzah AH, Pouraliakbar H, Bagheri R, Reihani SMS (2017) Al-Mg-Si/SiC laminated composites: fabrication, architectural characteristics, toughness, damage tolerance, fracture mechanisms. Compos Part B Eng 125:49–70

16. Chu K, Jia C, Jiang L, Li W (2013) Improvement of interface and mechanical properties in carbon nanotube reinforced Cu–Cr matrix composites. Mater Des 45:407–411

17. Monazzah AH, Pouraliakbar H, Bagheri R, Reihani SMS (2014) Toughness behavior in roll-bonded laminates based on AA6061/SiCp composites. Mater Sci Eng A 598:162–173

18. Kosa E, Göksenli A (2017) Influence of material hardness and particle velocity on erosive wear rate. J Mech Eng 47:9–15

19. Wang ZX, Wu HR, Shan XL, Lin NM, He ZY, Liu XP (2016) Microstructure and erosive wear behaviors of Ti6Al4V alloy treated by plasma Ni alloying. Appl Surf Sci 388:510–516

20. Harsha AP, Tewari US (2003) Two-body and three-body abrasive wear behaviour of polyaryletherketone composites. Polym Test 22:403–418

21. Bayer RG (2002) Fundamentals of wear failures. ASM Handb Vol 11, Fail Anal Prev 901–905

22. Zhou S, Zhao W, Xiong W (2009) Microstructure and properties of the cermets based on Ti (C, N). Int J Refract Met Hard Mater 27:26–32

23. Pan Z, Rupert TJ (2017) Mechanisms of near-surface structural evolution in nanocrystalline materials during sliding contact. Phys Rev Mater 1:43602

24. Avcu E, Fidan S, Yıldıran Y, Sınmazçelik T (2013) Solid particle erosion behaviour of Ti6Al4V alloy. Tribol Surf Interfaces 7:201–210

25. Wang H, Wang S, Gao P, Jiang T, Lu XG, Li CH (2016) Microstructure and mechanical properties of a novel near-α titanium alloy Ti6. 0Al4. 5Cr1. 5Mn. Mater Sci Eng A 672:170–174

26. Gofrey TMT, Goodwin PS, Ward-Close CM (2000) Titanium particulate metal matrix composites–Reinforcement, production methods, and mechanical properties. Adv Eng Mater 2:85–91

27. Rajan TPD, Pillai RM, Pai BC (1998) Reinforcement coatings and interfaces in aluminium metal matrix composites. J Mater Sci 33:3491–3503

28. Falodun OE, Oke SR, Obadele BA et al (2019) Influence of SiAlON ceramic reinforcement on Ti6Al4V alloy matrix via spark plasma sintering technique. Met Mater Int:1–10. https://doi.org/10.1007/s12540-019-00553-3

29. Feng H, Zhou Y, Jia D, Meng Q (2005) Rapid synthesis of Ti alloy with B addition by spark plasma sintering. Mater Sci Eng A 390:344–349

30. Falodun OE, Obadele BA, Oke SR, Maja ME, Olubambi PA (2018) Effect of sintering parameters on densification and microstructural evolution of nano-sized titanium nitride reinforced titanium alloys. J Alloys Compd 736:736–210. https://doi.org/10.1016/j.jallcom.2017.11.140

31. Muhammad M, Masoomi M, Torries B, Shamsaei N, Haghshenas M (2018) Depth-sensing time-dependent response of additively manufactured Ti-6Al-4V alloy. Addit Manuf 24:37–46

32. Ma X, Li F, Zhao C, Zhu G, Li W, Sun Z, Yuan Z (2017) Indenter load effects on creep deformation behavior for Ti-10 V-2Fe-3Al alloy at room temperature. J Alloys Compd 709:322–328

33. Batalha GF, Motyka M, Kubiak K, et al (2014) Editorial Board Contributors to Volume 2 Preface xv. Compr Mater Process

34. Batory D, Szymanski W, Panjan M et al (2017) Plasma nitriding of Ti6Al4V alloy for improved water erosion resistance. Wear 374:120–127

35. FALODUN OE, OBADELE BA, OKE SR et al (2018) Influence of spark plasma sintering on microstructure and wear behaviour of Ti-6Al-4V reinforced with nanosized TiN. Trans Nonferrous Met Soc China (English Ed 28). 47–54. https://doi.org/10.1016/S1003-6326(18)64637-0

36. Ghosh NC, Harimkar SP (2013) Microstructure and wear behavior of spark plasma sintered Ti3SiC2 and Ti3SiC2–TiC composites. Ceram Int 39:4597–4607

37. Russias J, Cardinal S, Aguni Y, Fantozzi G, Bienvenu K, Fontaine J (2005) Influence of titanium nitride addition on the microstructure and mechanical properties of TiC-based cermets. Int J Refract Met Hard Mater 23:358–362

38. Cardinal S, Malchere A, Garnier V, Fantozzi G (2009) Microstructure and mechanical properties of TiC–TiN based cermets for tools application. Int J Refract Met Hard Mater 27:521–527

39. Hussainova I, Kubarsepp J, Pirso J (2001) Mechanical properties and features of erosion of cermets. Wear 250:818–825

40. Reshetnyak H, Kuybarsepp J (1994) Mechanical properties of hard metals and their erosive wear resistance. Wear 177:185–193

41. Hussainova I (2003) Effect of microstructure on the erosive wear of titanium carbide-based cermets. Wear 255:121–128

42. Wentzel EJ, Allen C (1995) Erosion-corrosion resistance of tungsten carbide hard metals with different binder compositions. Wear 181:63–69

43. Neville A, McDougall BAB (2002) Electrochemical assessment of erosion-corrosion of commercially pure titanium and a titanium alloy in slurry impingement. Proc Inst Mech Eng Part L J Mater Des Appl 216:31–41

44. Mphahlele MR, Oke SR, Ige OO et al (2019) Effect of TiN nanoparticles on the friction and wear properties of spark plasma sintered Fe-Cr-Ni. Tribol Ind 41

45. Maja ME, Falodun OE, Obadele BA et al (2018) Nanoindentation studies on TiN nanoceramic reinforced Ti–6Al–4V matrix composite. Ceram Int 44:143–155. https://doi.org/10.1016/j.ceramint.2017.12.042

46. Ma Y, Peng GJ, Feng YH, Zhang TH (2017) Nanoindentation investigation on creep behavior of amorphous CuZrAl/nanocrystalline Cu nanolaminates. J Non-Cryst Solids 465:8–16

47. Bľanda M, Duszová A, Csanádi T, Hvizdoš P, Lofaj F, Dusza J (2015) Indentation hardness and fatigue of the constituents of WC–Co composites. Int J Refract Met Hard Mater 49:178–183

48. Hu J, Zhang W, Peng G, Zhang T, Zhang Y (2018) Nanoindentation deformation of refine-grained AZ31 magnesium alloy: indentation size effect, pop-in effect and creep behavior. Mater Sci Eng A 725:522–529

49. Sadeghian Z, Lotfi B, Enayati MH, Beiss P (2011) Microstructural and mechanical evaluation of Al–TiB2 nanostructured composite fabricated by mechanical alloying. J Alloys Compd 509:7758–7763

Publisher's note Springer Nature remains neutral with regard to jurisdictional claims in published maps and institutional affiliations.